AIAA 81-1555R

Model for Prediction of Double-Base Propellant Burn Rate, Including Cross-Flow Effects

Merrill K. King*
Atlantic Research Corporation, Alexandria, Virginia

A model permitting the prediction of mass burning rate of uncatalyzed NG/NC double-base propellants as a function of cross-flow velocity, pressure, and formulation heat of explosion has been developed. Two cross-flow model variants, differing in assumptions regarding the penetration of cross-flow induced turbulence into the fizz zone, were examined. In the first variant, the fizz zone was treated as being sufficiently structured to prevent turbulence penetration. This model variant was found to result in serious underprediction of cross-flow effects. In the other variant, the fizz zone was treated as a gas in terms of its fluid dynamic behavior, with resultant turbulence amplification of transport properties in both the fizz and dark zones. With this approach, reasonably good agreement between predicted and measured burning rates over a wide range of cross-flow velocities was obtained. Under zero-cross-flow conditions, the model was found to give good agreement with data for burning mass fluxes in excess of 0.5 g/cm^2-s without introduction of a pressure-dependency for surface/subsurface condensed-phase heat release. Inclusion of pressure dependency in this term permitted extension of the region of good agreement between data and theory down to 0.3 g/cm^2-s.

Nomenclature

A_S = pre-exponential in Arrenhius expression relating mass burning flux to surface temperature
b = blowing parameter, defined by Eq. (A2)
C_f = skin friction coefficient, with blowing
C_{f0} = nonblowing skin friction coefficient
C_{PDZ} = heat capacity in dark zone
C_{PFZ} = heat capacity in fizz zone
C_{PS} = condensed-phase propellant heat capacity
E_{FZ} = fizz zone reaction activation energy
E_S = surface reaction activation energy
h = flow channel half-height
H_{EX} = propellant heat of explosion
K_{FZRX} = fizz zone reaction constant, defined by Eq. (10)
L_{FZ} = fizz zone thickness
M = cross-flow Mach number
MW = molecular weight of propellant ablation products
$\dot{m}$ = propellant burning mass flux
P = pressure
Q_{FF} = heat release per unit mass in final flame
Q_{gas} = heat release per unit mass in fizz zone flame
Q_L = net surface/subsurface heat release per unit mass
R = gas law constant
T = temperature
T_0 = propellant conditioning temperature
T_{flame} = propellant adiabatic flame temperature
T_S = propellant surface temperature
T_{DZ} = dark zone temperature in absence of final flame influence
$T_{FZ\text{-}DZ}$ = temperature at fizz zone-dark zone interface
u = cross-flow velocity
U_{fs} = freestream cross-flow velocity
V = average (one-dimensional) cross-flow velocity
X = distance coordinate normal to propellant surface (Fig. 2)
ΔL_{FF} = dark zone thickness
$\mathfrak{D}$ = diffusivity of reactant R in the ambient gas
ϵ = eddy viscosity
λ, λ_L = molecular thermal conductivity of ablation products
λ_t = total (molecular plus turbulent) thermal conductivity
μ = molecular viscosity
ρ = gas density
τ = local shear stress
τ_{FZRX} = fizz zone reaction time
τ_{wall} = wall shear stress
ν = reaction order for fizz zone reaction

Presented as Paper 81-1555 at the AIAA/SAE/ASME 17th Joint Propulsion Conference, Colorado Springs, Colo., July 27-29, 1981; submitted Aug. 31, 1981; revision received Feb. 16, 1982. Copyright © American Institute of Aeronautics and Astronautics, Inc., 1981. All rights reserved.

*Chief Scientist, Research and Technology Division. Member AIAA.

Background

OVER the past twenty years, numerous models for prediction of solid propellant burning rate augmentation due to cross flow of combustion product gases across the propellant surface have been developed. Most of those developed prior to 1977 are referenced and reviewed in Ref. 1, while more recent models appear in Refs. 2-12. These models may be divided into several categories: 1) models based on heat transfer from a "core" gas to the propellant surface by forced convection; 2) models based on the alteration of transport properties between a gas-phase flame zone and the propellant surface by cross-flow-induced turbulence; 3) models based on chemically reacting boundary-layer theory; and, 4) models based on alteration of flame geometry by cross flow. Some of these models have been developed specifically for homogeneous propellants and others for heterogeneous propellants, while in some of the heat transfer models, the propellant type is not even considered. For the most part, these models emphasize the fluid dynamic aspects of the problem with little attention being paid to the combustion wave structure, a major shortcoming in this author's opinion. Recently, however, several models of composite propellant erosive burning (notably those of King,[2-4] Renie et al.,[5] and Lengelle[12]) with emphasis on the flame structure have been developed.

It does not appear to this writer that any of the existing homogeneous (double-base) propellant erosive burning models adequately treat the observed mechanistic details of

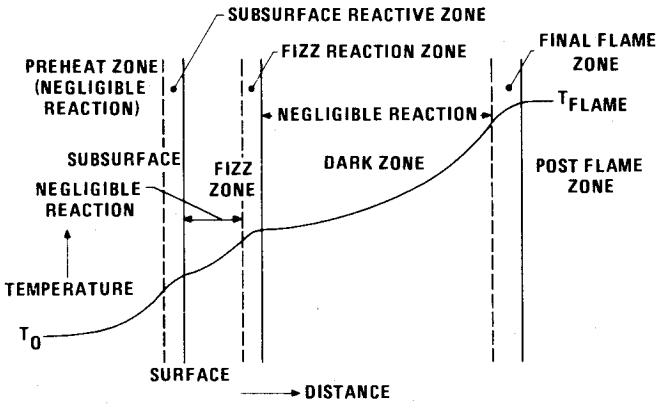

Fig. 1 Postulated double-base propellant flame structure.

double-base propellant combustion, notably the existence of multiple heat release regions separated by zones in which little reaction takes place. Instead, the existing models of double-base propellant erosive burning either simply treat forced convective heat transfer from the mainstream core flow to the propellant surface or, at best, analyze heat feedback from a single flame zone whose location is defined by analysis of one simple global reaction. In the current effort, the effects of cross flow on a multiple-flame double-base propellant combustion wave as described by Rice and Ginnell,[13] among others, are examined.

The proposed double-base propellant flame structure is depicted in Fig. 1. As indicated, there are three major reaction zones, separated by regions in which negligible reaction occurs, sometimes referred to as induction zones. Deep below the surface, the propellant is simply preheated from its conditioning temperature until it reaches a temperature, near the surface, at which reaction to preliminary gaseous or gas/liquid spray products takes place. These fragments are further heated by the thermal wave until a second set of reactions producing NO and simple organic molecules (notably formaldehyde) occurs in a second reaction zone (which may be quite thin or may occupy a large fraction of the fizz zone, depending on the temperature sensitivity of the reaction rates). Finally, there is a long induction zone, generally referred to as the "dark zone," terminated by a final luminous flame zone in which the intermediates are converted to equilibrium products. It is generally claimed that this last reaction zone is quite thin, allowing it to be reasonably approximated as a flame sheet.

As indicated in Fig. 1, the second derivative of temperature is positive in the nonreactive regions and negative in the reaction zones. In the absence of cross flow, it may be easily shown that the long distance separating the final flame zone from the fizz zone, combined with the relatively low gas molecular conductivity results in negligible heat feedback from the final flame zone to the inner zones, thus causing the temperature-distance derivative to be essentially zero at the inner edge of the dark zone, with resultant decoupling of the final flame zone processes from the burn-rate-controlling fizz zone and subsurface zone reaction processes. However, in the presence of strong cross flow, induced turbulence can cause the average effective turbulent thermal conductivity across the dark zone to be raised one to two orders of magnitude above the molecular thermal conductivity. Preliminary calculations performed using empirical expressions for the dark zone width based on the work of Aoki and Kubota[14] indicate that such an increase results in the final flame region contributing appreciable heat flux back to the fizz zone, thus raising its temperature markedly. This, in turn, accelerates the reactions in this zone causing greatly increased heat feedback to the propellant surface with a resultant increase in burning rate.

A second potential mechanism by which cross flow can accelerate the burning rate of homogeneous double-base propellants involves possible penetration of cross-flow-induced turbulence into the fizz zone with resultant increase in heat feedback from the fizz zone reaction region to the propellant surface. However, due to the observed gas/liquid froth structure of this zone, it is not totally clear how effectively cross-flow-induced turbulence will penetrate through this zone toward the propellant surface. Accordingly, two limiting-case analyses have been developed and are presented: 1) no turbulence penetration into the fizz zone, with the outer edge of the fizz zone being considered to be an effective surface as regards the flowfield analysis; and, 2) treatment of the fizz zone as a pure gas, with the flowfield analysis beginning at the actual propellant surface.

Model Development

The model development was carried out in two phases. First, several fairly closely related models were developed for the combustion of homogeneous double-base propellants in the absence of cross flow. These models were tested against a data base developed by Miller et al.,[15] and one was selected for extension to treatment of cross-flow effects. As mentioned previously, two separate erosive burning models, representing limiting cases as regards penetration of cross-flow-induced turbulence into the fizz zone, were then developed.

As indicated earlier, in the pressure range of practical interest, the final flame zone is sufficiently far from the propellant surface that under no-cross-flow conditions it does not affect the propellant burning rate, with heat feedback from it to the fizz zone being negligible and the temperature gradient at the inner edge of dark zone being zero.

In the first variant of the no-cross-flow model, the fizz reaction zone is assumed to be infinitesimally thin (flame sheet) with its distance from the surface being calculated as the product of the velocity of gas flow from the surface and a characteristic reaction time. Based on the work of Beckstead,[16] it is assumed that the burning mass flux and surface temperature are related by

$$\dot{m} = A_S e^{-E_S/RT_S}$$

$$A_S = 5000 \text{ g/cm}^2 \text{ s}$$

$$E_S = 10{,}000 \text{ cal/g-mole} \tag{1}$$

Since there is no heat release between the surface and the fizz zone flame sheet (located at $X = L_{FZ}$), then between $X = 0$ and $X = L_{FZ}$

$$\lambda \frac{d^2T}{dX^2} - \dot{m} C_{PFZ} \frac{dT}{dX} = 0 \tag{2}$$

At $X = L_{FZ}$, with application of an energy balance and use of the fact that the temperature gradient is zero at the inner edge of the dark zone

$$T = T_{DZ} \tag{3}$$

$$\lambda \frac{dT}{dX}\bigg|_{X=L_{FZ}} = \dot{m} Q_{gas} \tag{4}$$

where T_{DZ} is the dark zone temperature and Q_{gas} the heat release per unit mass in the fizz zone flame sheet. Application of an overall energy balance (with zero feedback from the final flame) yields

$$Q_{gas} = C_{PFZ}(T_{DZ} - T_S) + C_{PS}(T_S - T_0) - Q_L \tag{5}$$

where T_0 is the propellant conditioning temperature and Q_L the net surface/subsurface heat release per unit mass of propellant. Integration of Eq. (2), application of the boundary conditions given by Eqs. (3) and (4), and substitution of

Eq. (5) yields

$$T_S = T_{DZ} - \left[(T_{DZ} - T_S) + \frac{C_{PS}}{C_{PFZ}} (T_S - T_0) - \frac{Q_L}{C_{PFZ}} \right] \times (1 - e^{-\dot{m} C_{PFZ} L_{FZ}/\lambda}) \quad (6)$$

At this point, expressions for T_{DZ}, Q_L, and L_{FZ} are needed for closure of the problem.

Aoki and Kubota[14] have recently published results of experimental determination of dark zone temperature as a function of pressure and formulation heat of explosion (H_{EX}) for a series of double-base propellants containing nitrocellulose (12.2% N), nitroglycerine, diethylphthalate, and 2-nitrodiphenylamine in varying ratios; their data may be fit reasonably well by

$$T_{DZ} = a + dH_{EX}$$

$$d = 0.425$$

$$a = 720 + 125 \ell n(P), \quad P \leq 20 \text{ atm (2 MPa)}$$

$$a = 855 + 80 \ell n(P), \quad P > 20 \text{ atm (2 MPa)} \quad (7)$$

with P in atmospheres.

Two expressions for Q_L were examined in the course of this study. The first of these, taken from the work of Beckstead,[16] relates Q_L to H_{EX} alone

$$Q_L = 65.7 + 0.013 H_{EX} \quad (8a)$$

with H_{EX}, Q_L in cal/g. As will be discussed later, this expression yielded excellent agreement between burning rate predictions and data at high pressures but led to a pressure exponent of zero at low pressures, in conflict with the data, due to lack of pressure dependency of Q_L. [At sufficiently low pressures, less than approximately 10-20 atm (1-2 MPa), depending on the value of H_{EX}, the burning becomes driven by the surface/subsurface heat release, with gas-phase feedback from the fizz zone going to zero.] Accordingly, a modified expression, allowing for dependence of Q_L on pressure (with parametric variation of the exponential pressure dependency to optimize agreement between theory and data), was utilized

$$Q_L = (65.7 + 0.013 H_{EX})(P/6)^{0.08} \quad (8b)$$

with P in atmospheres. [Interestingly enough, subsequent to development of this model, the author found a report by Kubota et al.[17] in which thermocouple measurements of temperature profiles in burning double-base propellants were used in combination with surface heat balances for estimation of surface heat release as a function of burning rate. Combining their data for uncatalyzed formulations with burning rate vs pressure data for the same formulations (Figs. 10, 19, and 52 of Ref. 17) yields a plot of Q_L vs pressure which indicates that Q_L is approximately proportional to pressure to the 0.10 power over a range of 1-100 atm (0.1-10.0 MPa), quite close to the pressure dependency expressed in Eq. (8b).]

Finally, the distance from the propellant surface to the fizz zone flame sheet (L_{FZ}) was calculated as the product of the average gas velocity across the fizz zone and a characteristic reaction time, given by the following equations.

$$V = \frac{\dot{m} R (T_{DZ} + T_S)}{2P(\text{MW})} \quad (9)$$

$$\tau_{FZRX} = \frac{K_{FZRX} e^{E_{FZ}/RT_{DZ}}}{T_{DZ} P^{(\nu - 1)}} \quad (10)$$

Based on the work of Aoki and Kubota[14] and Beckstead,[16] E_{FZ} was set equal to 40,000 and the reaction order ν was chosen to be unity. With these substitutions, Eqs. (9) and (10) may be combined to yield

$$L_{FZ} = \frac{\dot{m} R K_{FZRX} (T_{DZ} + T_S) e^{40{,}000/RT_{DZ}}}{2P(\text{MW}) T_{DZ}} \quad (11)$$

where K_{FZRX} is the fizz zone global reaction rate pre-exponential, which is determined by fitting one data point out of the Miller[15] burning rate data base for NC (12.6% N)/NG/secondary plasticizer double-base formulations. (Since burning rate is observed to depend on the degree of nitration of nitrocellulose, this constant would probably change for formulations containing NC with different levels of nitration, such as JPN with its 13.5% N nitrocellulose.)

Substitution of Eqs. (7) and (8) into Eqs. (6) and (11) reduces the problem to three equations [Eqs. (1), (6), and (11)] with three unknowns ($\dot{m}$, L_{FZ}, and T_S) which are simply solved (though care must be taken in low pressure cases where the gas-phase heat feedback becomes negligible), to give burning rate as a function of pressure and formulation heat of explosion.

In a second approach to the analysis of no-cross-flow double-base propellant combustion, it was assumed that the volumetric heat release is distributed uniformly across the entire fizz zone. In this case, Eq. (2) is replaced by

$$\lambda \frac{d^2 T}{dX^2} - \dot{m} C_{PFZ} \frac{dT}{dX} + \dot{Q} = 0 \quad (12)$$

where

$$\dot{Q} = \frac{\dot{m}}{L_{FZ}} [C_{PFZ}(T_{DZ} - T_S) + C_{PS}(T_S - T_0) - Q_L] \quad (13)$$

and the boundary condition given by Eq. (4) is replaced by

$$\left. \frac{dT}{dX} \right|_{X = L_{FZ}} = 0 \quad (14)$$

Integration of Eq. (12) followed by application of the boundary conditions given by Eqs. (3) and (14) yields

$$T_S = T_0 + \frac{Q_L}{C_{PS}} + \frac{\lambda}{\dot{m} C_{PS} L_{FZ}} \left[(T_{DZ} - T_S) + \frac{C_{PS}}{C_{PFZ}} (T_S - T_0) - \frac{Q_L}{C_{PFZ}} \right] (1 - e^{-\dot{m} C_{PFZ} L_{FZ}/\lambda}) \quad (15)$$

as a replacement for Eq. (6). The remainder of the analysis is identical with that of the first model variant.

The third model variant examined employed the Zeldovich approach to flame-speed calculations, with division of the fizz zone into a conductive-convective region with no reaction and a conductive-reactive region in which convection is neglected. Details of this type of analysis are presented in a text by Glassman[18] and will not be repeated here. For a first-order gas-phase reaction, this analysis results in the following relationship between burning mass flux, dark zone temperature, surface temperature, and surface/subsurface heat release:

$$\dot{m} = \sqrt{\frac{2 K_{FZRX} \lambda T_{DZ}^2 (e^{-40{,}000/RT_{DZ}}) P}{C_{PFZ}(T_{DZ} - T_S) + C_{PS}(T_S - T_0) - Q_L}} \quad (16)$$

which may be combined with Eqs. (1), (7), and (8) for calculation of burning rate as a function of pressure and formulation heat of explosion. [It should be noted that Eq.

(16) becomes invalid if the surface temperature drops below a value given by $C_{PS}(T_S - T_0) = Q_L$; in this case, condensed-phase heat release controls and the burning rate is found by setting $T_S = Q_L/C_{PS} + T_0$ and substituting this value of T_S into Eq. (1).]

Finally, a fourth no-cross-flow model variant using an eigenvalue problem approach as described subsequently was developed. In this approach, the fizz zone reactions were assumed to be represented by a single global first-order Arrenhius kinetics reaction. As before, Eq. (1) was employed to relate the mass burning flux to surface temperature, and Eqs. (5), (7), and (8) were used for calculation of T_{DZ}, Q_L, and, finally, Q_{gas} as a function of surface temperature. Energy and species mass balances within the fizz zone yield

$$\lambda \frac{d^2T}{dX^2} - \dot{m}C_{PFZ}\frac{dT}{dX} + \dot{q} = 0 \tag{17}$$

$$\mathcal{D}\rho \frac{d^2y_R}{dX^2} - \dot{m}\frac{dy_R}{dX} - \dot{w}_R = 0 \tag{18}$$

where y_R is the mass fraction of reactant R, $\dot{w}_R$ the volumetric rate of depletion of reactant R, and $\dot{q}$ the volumetric heat release rate. The Shvab-Zeldovich[19] approach was then used to develop a relationship between $y_R(X)$ and $T(X)$

$$y_R = \frac{C_{PFZ}y_{R_{init}}}{Q_{gas}}[T_{DZ} - T] \tag{19}$$

where $y_{R_{init}}$ is the mass fraction of material leaving the surface which is reactant R. With the assumption of first-order kinetics, the volumetric heat release rate may be expressed as

$$\dot{q} = A_g Q_{gas} e^{-E_g/RT} P y_R / T \tag{20}$$

Combining Eqs. (17), (19), and (20), using $E_g = 40{,}000$ cal/mole (again based on the work of Aoki and Kubota[14] and Beckstead[16]), and lumping the product of A_g and $y_{R_{init}}$ into one constant to be evaluated by fitting one data point, one obtains

$$\lambda \frac{d^2T}{dX^2} - \dot{m}C_{PFZ}\frac{dT}{dX} + \frac{A_g' P C_{PFZ} e^{-40{,}000/RT}(T_{DZ} - T)}{T} = 0 \tag{21}$$

with boundary conditions

$$\dot{m}[C_{PFZ}(T_S - T_0) - Q_L] = \lambda \frac{dT}{dX}\bigg|_{X=0^+} \tag{22}$$

$$T = T_{DZ} \quad \text{at} \quad X \to \infty \tag{23}$$

For a given pressure and formulation heat of explosion, the following procedure is used to calculate a predicted burning mass flux. First, a value of surface temperature is guessed and Eqs. (1), (5), (7), (8), and (22) are used to calculate $\dot{m}$, Q_{gas}, T_{DZ}, Q_L, and dT/dX at $X = 0^+$. Equation (21) is then integrated, using the $X = 0$ values of T and dT/dX, by a Runge-Kutta procedure out toward $X = \infty$. If T climbs above T_{DZ}, the calculation is terminated and a lower value of surface temperature guessed, while if the temperature derivative turns negative before T_{DZ} is reached, the calculation is terminated and a higher value of surface temperature is guessed; this procedure being repeated until the surface temperature is bracketed within 0.5 K (corresponding to an error band of approximately 1% on burning rate).

As will be discussed in the next section, all four zero-cross-flow model variants have been found to give comparable predictions of the Miller[15] data base for burning rate as a function of pressure and heat of explosion. Accordingly, the first variant (with pressure-dependent Q_L) was selected on the basis of its relative simplicity for extension to the case of nonzero cross flow. As mentioned earlier, two cross-flow models have been developed: in the first, the fizz zone is assumed to be structurally rigid, with no penetration of turbulence into it; while in the second, the fizz zone has been treated as a gas in terms of its fluid dynamic behavior.

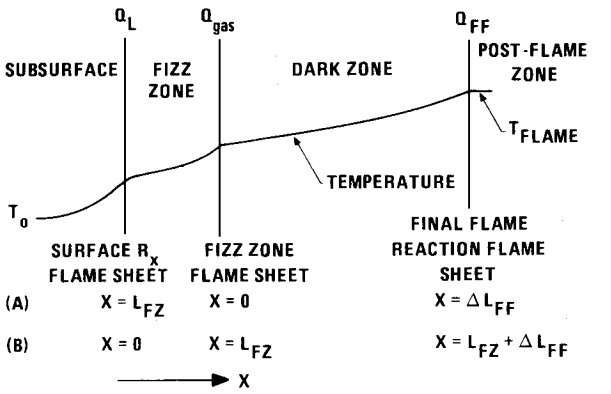

Fig. 2 Double-base propellant erosive burning model; a) coordinate system used for rigid fizz zone model and b) coordinate system used for gaseous fizz zone model.

A sketch of the postulated flame structure for both cross-flow models is presented as Fig. 2. For convenience in applying a boundary-layer analysis computer code previously developed for modeling of composite propellant erosive burning,[2-4] the coordinate system for the first (rigid fizz zone) model is chosen such that the origin ($X = 0$) is at the interface of the dark zone and the fizz zone since in this model this interface is the "surface" of the propellant as regards the flow analysis. As may be seen, there are three distinct infinitesimally thin (flame sheet) heat release zones separated by regions of negligible heat release. (As long as activation energies associated with the key heat release reactions are reasonably high the flame sheet approximation is good for cross-flow as well as no-cross-flow situations for this premixed flame situation.) As in the zero-cross-flow case, mass burning flux is related to the surface ($X = -L_{FZ}$) temperature through Eq. (1). In addition, it may be shown that the heat release at the fizz zone flame sheet is given by

$$Q_{gas} = C_{PFZ}(a + dH_{EX} - T_S) + C_{PS}(T_S - T_0) - Q_L \tag{24}$$

with Q_L given by Eq. (8a). Integration of the Fourier equation with no heat release between $X = -L_{FZ}$ and $X = 0$, followed by application of boundary conditions at $X = 0$:

$$T = T_{FZ\text{-}DZ} \quad \text{at} \quad X = 0 \tag{25}$$

$$\lambda \frac{dT}{dX}\bigg|_{X=0^-} = \dot{m}Q_{gas} + \lambda \frac{dT}{dX}\bigg|_{X=0^+} \tag{26}$$

leads to

$$T_S = T_{FZ\text{-}DZ} - \left[\frac{Q_{gas}}{C_{PFZ}} + \frac{\lambda}{\dot{m}C_{PFZ}}\frac{dT}{dX}\bigg|_{X=0^+}\right](1 - e^{-\dot{m}C_{PFZ}L_{FZ}/\lambda}) \tag{27}$$

(It should be noted that $T_{FZ\text{-}DZ}$ is not the same as T_{DZ} used previously in the no-cross-flow analysis, due to heat feedback from the final flame causing an increase in this temperature.) L_{FZ} is calculated using the same equation form as Eq. (11), with $T_{FZ\text{-}DZ}$ replacing T_{DZ}

$$L_{FZ} = \frac{\dot{m}RK_{FZRX}(T_{FZ\text{-}DZ} + T_S)e^{40{,}000/RT_{FZ\text{-}DZ}}}{2P(MW)T_{FZ\text{-}DZ}} \tag{28}$$

Data presented by Aoki and Kubota[14] regarding dark zone dimensions were used to develop the following expression for the dark zone thickness.

$$\Delta L_{FF} = \frac{252}{P^{2.1}} \left(\frac{\dot{m}}{\dot{m}_{\text{no cross flow}}} \right) \tag{29}$$

where pressure is in atmospheres and ΔL_{FF} in centimeters. An overall energy balance is used to develop an expression for the final flame heat release

$$Q_{FF} = C_{PDZ}(T_f - a - dH_{EX}) \tag{30}$$

where the flame temperature T_f is calculated from thermodynamic equilibrium considerations. For closure of the problem, expressions for $T_{FZ\text{-}DZ}$ and $(dT/dX)\,|_{X=0^+}$ are required. Due to turbulence in the dark zone induced by cross flow, the effective (turbulent plus molecular) thermal conductivity varies strongly across this zone. Accordingly, the transport of energy across this zone is best calculated by breaking the zone up into many segments, over each of which effective thermal conductivity is nearly constant, solving the Fourier equation for each segment and applying boundary condition matching conditions at each segment interface. This procedure results in

$$T_{FZ\text{-}DZ} = T_{\text{flame}} - \frac{Q_{FF}}{C_{PDZ}} \left[1 - \prod_{N=1}^{N=NTOT} \exp\{ -\dot{m} C_{PDZ} [X(N) - X(N-1)]/\lambda_t(N) \} \right] \tag{31}$$

$$\left. \frac{dT}{dX} \right|_{X=0^+} = \frac{\dot{m} Q_{FF}}{\lambda_t(N=1)} \left[\prod_{N=1}^{N=NTOT} \exp\{ -\dot{m} C_{PDZ} [X(N) - X(N-1)]/\lambda_t(N) \} \right] \tag{32}$$

where $N=1$ at $X=0$, $N=NTOT$ at $X=\Delta L_{FF}$ and the values of effective thermal conductivity λ_t are calculated as a function of position using a turbulent boundary-layer analysis procedure described in Refs. 2-4, and briefly outlined in the Appendix.

The following procedure is used to solve the preceding equations for burning mass flux at a given pressure, cross-flow velocity, and formulation heat of explosion. First, the no-cross-flow analysis is used to calculate the base burning mass flux for the given pressure and heat of explosion values. A value of $\dot{m}$ is then guessed and Eq. (29) is used to calculate ΔL_{FF}. Equation (30) is then used to calculate Q_{FF} and the flow profile analysis together with Eqs. (31) and (32) are used to evaluate $T_{FZ\text{-}DZ}$ and $(dT/dX)\,|_{X=0^+}$. Equation (1) is next solved for T_S, and Eq. (24) for Q_{gas}, after which Eqs. (27) and (28) are solved simultaneously for L_{FZ} and $\dot{m}$. The calculated $\dot{m}$ is then checked against the previous value, a new value is guessed, and the procedure is repeated to convergence.

For the second (gaseous fizz zone) erosive burning model, because the boundary-layer analysis must begin at the propellant surface, the coordinate system is redefined so that the origin is at the actual propellant surface (Fig. 2b). The equation development for the model is essentially the same as for the rigid fizz zone model, except that in this case allowance must also be made for variation in effective thermal conductivity across the fizz zone as well as across the dark zone. This change results in replacement of Eq. (27) by

$$T_S = T_{FZ\text{-}DZ} - \left[\frac{Q_{gas}}{C_{PFZ}} + \frac{\lambda_{t,X=L_{FZ}}}{\dot{m} C_{PFZ}} \left. \frac{dT}{dX} \right|_{X=L_{FZ}^+} \right] \times \left(1 - \prod_{M=1}^{M=MTOT} \exp\{ -\dot{m} C_{PFZ} [X(M) - X(M-1)]/\lambda_t(M) \} \right) \tag{33}$$

where $M=1$ at $X=0$, $M=MTOT$ at $X=L_{FZ}$ and Eqs. (31) and (32) are replaced by

$$T_{FZ\text{-}DZ} = T_{\text{flame}} - \frac{Q_{FF}}{C_{PDZ}} \left[1 - \prod_{N=1}^{NTOT} \exp\{ -\dot{m} C_{PDZ} [X(N) - X(N-1)]/\lambda_t(N) \} \right] \tag{34}$$

$$\left. \frac{dT}{dX} \right|_{X=L_{FZ}^+} = \frac{\dot{m} Q_{FF}}{\lambda_t(N=1)} \left[\prod_{N=1}^{NTOT} \exp\{ -\dot{m} C_{PDZ} [X(N) - X(N-1)]/\lambda_t(N) \} \right] \tag{35}$$

and $N=1$ at $X=L_{FZ}$, $N=NTOT$ at $X=L_{FZ}+\Delta L_{FF}$. The equation solution procedure is basically unchanged.

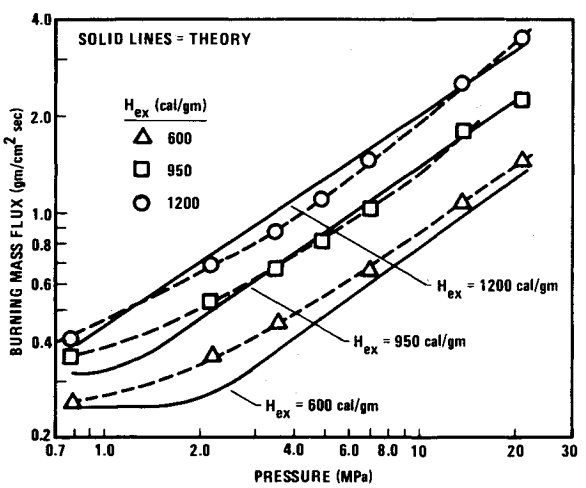

Fig. 3 Comparison of predicted burning rates using a flame-sheet model with Miller data (surface/subsurface heat release independent of pressure).

Results and Discussion

As mentioned earlier, Miller[15] has generated a systematic data base for burning rate of nitrocellulose (12.6% N)/nitroglycerine/secondary plasticizer double-base formulations as a function of pressure and heat of explosion, without cross flow. Each of the no-cross-flow model variants described in the previous section has been used to predict the dependence of burn rate on pressure and H_{EX} for these formulations, with one point of the data base being used to fix the one unknown constant, the fizz zone reaction rate pre-exponential, in each variant. For the flame sheet, uniformly distributed heat release, and Zeldovich approach variants, the base point used was at $P=35$ atm (3.5 MPa), $H_{EX}=950$ cal/g, while for the eigenvalue approach, it was at $P=49$ atm (4.9 MPa), $H_{EX}=950$ cal/g. Predicted and measured burning mass fluxes for three of the variants are presented in Figs. 3-7. In the first three of these figures, the surface/subsurface heat release parameter was assumed to be pressure independent, while in the latter two figures it was allowed to depend on pressure in accordance with Eq. (8b). As may be seen from Figs. 3-5, the three model variants with pressure-independent surface heat release give reasonably good predictions of data for the higher

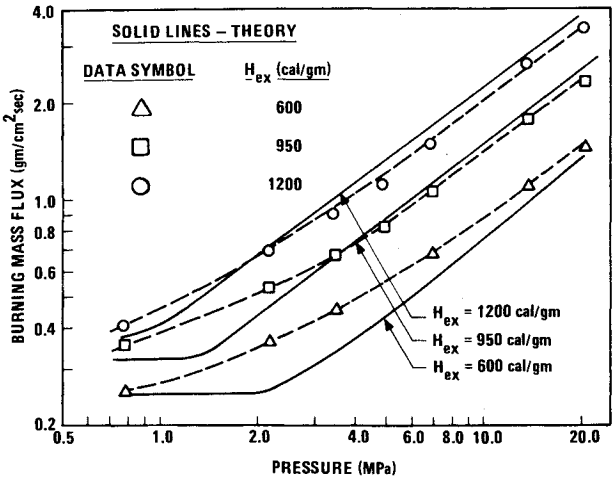

Fig. 4 Comparison of predicted burning rates using a Zeldovich flame model with Miller data (surface/subsurface heat release independent of pressure).

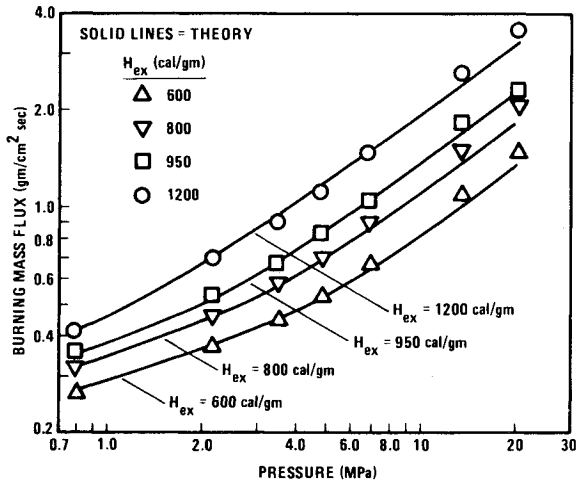

Fig. 6 Comparison of predicted burning rates using a flame-sheet model with Miller data (pressure-dependent surface/subsurface heat release).

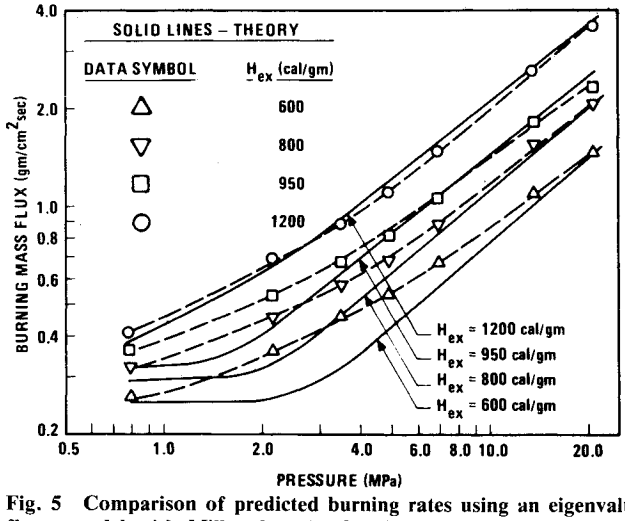

Fig. 5 Comparison of predicted burning rates using an eigenvalue flame model with Miller data (surface/subsurface heat release independent of pressure).

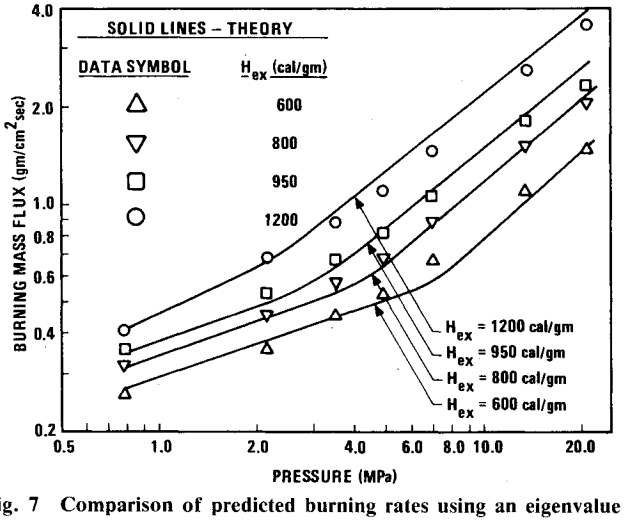

Fig. 7 Comparison of predicted burning rates using an eigenvalue flame model with Miller data. (pressure-dependent surface/subsurface heat release).

pressure end of the data band, but deviate somewhat at low pressure. The pressure at which the deviation occurs appears to increase with decreasing propellant heat of explosion. On the whole, the flame sheet and eigenvalue variants appear to do better than the Zeldovich-type model, while the uniform heat release approach (results not presented) does slightly worse. The explanation for the relatively poor agreement between theory and data at low pressure lies in the fact that at these lower pressures the burning begins to be driven totally by the surface/subsurface heat release, the offset distance of the fizz zone flame being so large as to provide negligible heat feedback to the surface. Since the surface/subsurface heat release was assumed to be pressure independent this of course leads to a predicted burning rate pressure exponent of zero in these low-pressure regions, at variance with experimental observations.

Accordingly, revised versions of the flame sheet and eigenvalue model variants, with allowance for pressure-dependent surface heat release [in accordance with Eq. (8b)] were developed and tested against the Miller data base. Results of these calculations are presented in Figs. 6 and 7. As may be seen, agreement between predicted and experimental burning rates is excellent with either model.

In Fig. 8, predictions made with the flame sheet model, with allowance for pressure-dependent surface/subsurface heat release in accordance with Eq. (8b), are compared against data obtained by Aoki and Kubota for two propellants with much higher NC/NG ratios than those tested by Miller. No constants were adjusted in making these predictions. As may be seen, at the higher pressures the agreement between data and predictions is excellent. However, at the low end of the pressure range examined, particularly for the lower energy formulation, theory and data diverge somewhat, with the model predicting higher burning rates than observed. The break between data and theory occurs at a burning mass flux of about 0.3 g/cm^2 s for each formulation. Examination of intermediate output from the model indicates that it is in this region that the condensed phase processes begin to control the burning rate, the gas phase flame moving so far away from the surface as to have no effect on burning rate at lower pressures. Thus, it appears that for improvement of the no-cross-flow model in the low pressure regime, effort will have to be concentrated on better modeling of the condensed phase processes.

The two erosive burning models developed (one assuming essentially a rigid fizz zone structure with no turbulent transport property augmentation in this region, the other assuming that the fizz zone acts like a gas in terms of penetration of turbulence) have been tested against data obtained for two NG/NC propellants by Burick and Osborn.[20] These formulations, designated as BUU and BDI, have heats of explosion of approximately 1050 cal/g and 920 cal/g, respec-

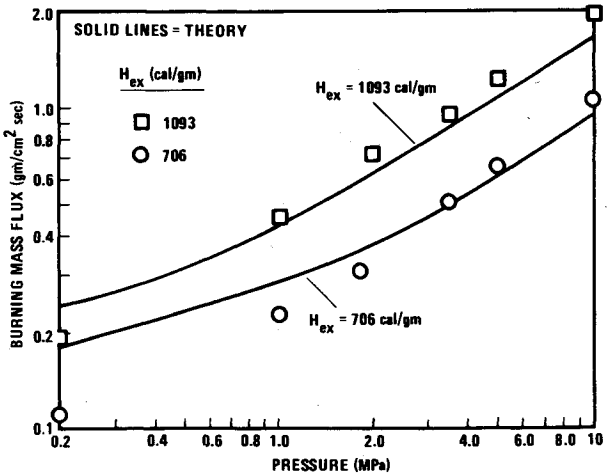

Fig. 8 Comparison of predicted burning rates using a flame-sheet model with data of Aoki and Kubota (pressure-dependent surface/subsurface heat release).

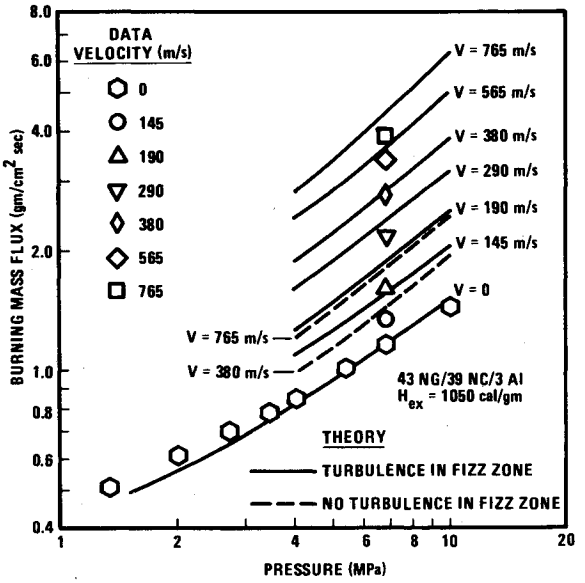

Fig. 9 Predicted and observed burning mass fluxes for BUU propellant.

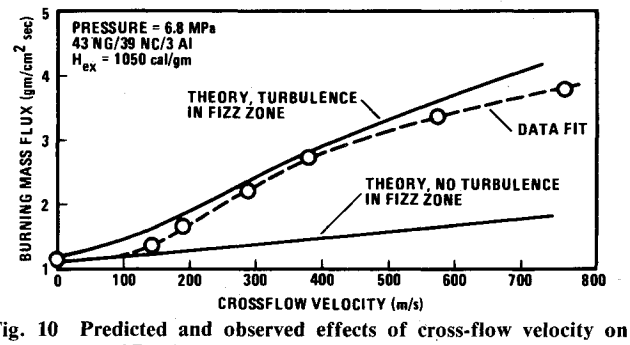

Fig. 10 Predicted and observed effects of cross-flow velocity on burning rate of BUU propellant.

tively. Predicted and observed burning mass fluxes are presented in Figs. 9-12. As may be seen from Fig. 9, the no-cross-flow predictions of burning rate vs pressure for BUU are excellent. In addition, the erosive burning predictions made assuming full turbulence penetration through the fizz zone are quite good, while the rigid structure fizz zone model results in drastic underprediction of the effects of cross flow.

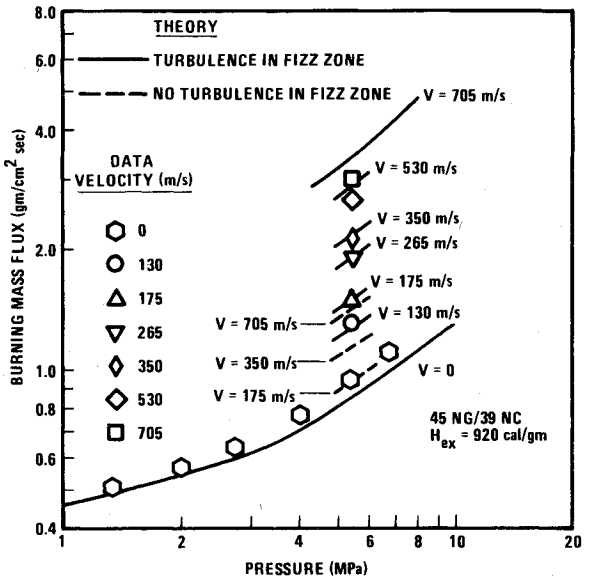

Fig. 11 Predicted and observed burning mass fluxes for BDI propellant.

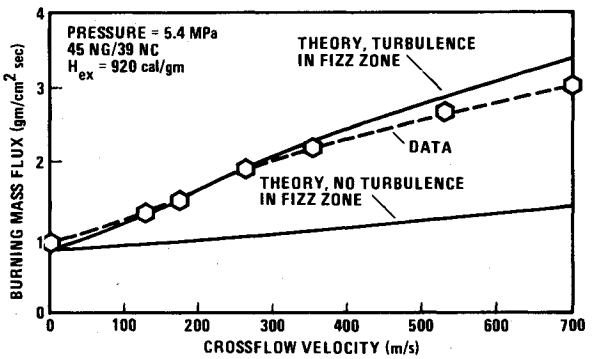

Fig. 12 Predicted and observed effects of cross flow on burning rate of BDI propellant.

This is more clearly shown in Fig. 10, where the burning mass flux (predicted and observed) is plotted against cross-flow velocity at constant pressure. As may be seen, the effects of cross flow predicted assuming turbulent boundary-layer development starting at the interface of the unburned propellant and the fizz zone agree quite well with data, while the alternative assumption regarding turbulence penetration into the fizz zone fails badly. Similar results for the BDI formulation appear in Figs. 11 and 12.

Summary

Several variants of a model for prediction of burning rate of uncatalyzed homogeneous double-base propellants as a function of pressure and heat of explosion, in the absence of cross flow, have been developed and shown to give reasonable agreement with data, particularly for burn rates in excess of approximately 0.5 g/cm² s. Allowance for pressure dependence of exothermic surface/subsurface reactions extends the region of good agreement between data and theory down to mass burning fluxes of approximately 0.3 g/cm² s (0.2 cm/s). One of the model variants developed, a flame-sheet model, has been extended to allow for the effects of cross flow. Two variants of a cross-flow model have been developed. In one of these, it is assumed that cross-flow-induced turbulence does not penetrate the fizz zone and that the only mechanism leading to increased burning in the presence of cross flow is turbulence augmentation of transport properties in the dark zone resulting in significant heat feedback from the final flame, which does not come into play in the absence of cross

flow. In the other variant, it is assumed that the fizz zone acts like a gas in terms of its fluid dynamic behavior, with cross-flow-induced turbulence not only bringing the final flame into play but also increasing the effective transport properties across the fizz zone. The latter variant is found to result in good agreement between predictions and data, while the former variant results in marked underprediction of the effects of cross flow on double-base propellant burning rate.

Appendix: Boundary-Layer Analysis for Determination of Effective Thermal Conductivity Distribution

Details of the boundary-layer analysis employed to determine distribution of total (molecular plus turbulent) thermal conductivity through the zones of interest are described in detail in Refs. 2-4; a brief outline and summary is presented next.

First the nonblowing skin friction coefficient is calculated as a function of cross-flow Reynolds number from a smooth-wall equation

$$C_{f0} = 0.00140 + 0.125 Re^{-0.32} \tag{A1}$$

(Options for treatment of a rough surface are also included in the analysis but were not invoked in this study.) The estimated mass burning flux (or value obtained in the previous calculation loop) is then used to generate the value of the blowing parameter b

$$b = \frac{2\dot{m}}{(\rho U_{\rm fs})_{\rm cross\ flow} C_{f0}} \tag{A2}$$

which is then used in calculation of the actual skin friction coefficient in the presence of blowing. Several optional equations for this parameter are included in the program; the one employed in the calculations presented herein (selected on the basis of success with prediction of composite propellant erosive burning) is

$$C_f = C_{f0} \left[1 - \frac{b}{10}\right]^2 \Big/ \left[1 + \frac{b}{10}\right]^{0.4} \tag{A3}$$

This value was then used to calculate a shear stress at the surface via

$$\tau_{\rm wall} = (C_f/2)\rho_{\rm fs} U_{\rm fs}^2 \tag{A4}$$

Application of a momentum integral analysis for a two-dimensional channel yields the following expression for local shear stress as a function of distance from the propellant surface and the local cross-flow velocity:

$$\tau = \tau_{\rm wall} + \dot{m}u - Kx \tag{A5}$$

$$K = 0.9\dot{m}\bar{U}\left[2 + \frac{(\gamma+1)M^2}{1-M^2}\right]\Big/ h \tag{A6}$$

(A similar expression may be derived for axisymmetric channel flow.) In addition, the local shear stress is related to the local cross-flow velocity gradient by

$$\tau = (\mu + \rho\epsilon)\,{\rm d}u/{\rm d}x \tag{A7}$$

A Prandtl mixing length expression for eddy viscosity

$$\epsilon = 0.168 X^2 ({\rm DF})^2 {\rm d}u/{\rm d}x \tag{A8}$$

and equations of state relating ρ and μ to temperature were employed along with the approximation of a linear temperature gradient across the zone of interest to close the analysis. (In the calculations presented in this paper, the damping factor DF was set equal to unity.)

With these relationships, Eqs. (A5-A8) may be combined and integrated from the wall (with $u=0$ at $X=0$ as a starting boundary condition) to yield among other things, the variation of eddy viscosity (ϵ) with X. The total (molecular plus turbulent) thermal conductivity may then be calculated as a function of X from

$$\frac{\lambda_t}{\lambda_L} = 1 + \frac{\rho\epsilon}{\mu} = f(x) \tag{A9}$$

Acknowledgments

Research was sponsored by the Air Force Office of Scientific Research (AFSC), United States Air Force, under Contract F49620-78-C-0016.

References

[1] King, M. K., "A Model of Erosive Burning of Composite Propellants," *Journal of Spacecraft and Rockets*, Vol. 15, May 1978, pp. 139-146.

[2] King, M. K., "A Model of the Effects of Pressure and Crossflow Velocity on Composite Propellant Burning Rate," AIAA Paper 79-1171, June 1979.

[3] King, M. K., "Experimental and Theoretical Study of the Effects of Pressure and Crossflow Velocity on Composite Propellant Burning Rate," *18th Symposium (International) on Combustion*, The Combustion Institute, Pittsburgh, Pa., 1981, pp. 207-216.

[4] King, M. K., "Predicted and Measured Effects of Pressure and Crossflow Velocity on Composite Propellant Burning Rate," *17th JANNAF Combustion Meeting*, CPIA Pub. 329, Vol. I, Nov. 1980, pp. 99-122.

[5] Renie, J. P., Condon, J. A., and Osborn, J. R., "Oxidizer Size Distribution Effects on Propellant Combustion," AIAA Paper 78-981, July 1978.

[6] Parkinson, R. C., "Erosive Burning as a Boundary Layer Phenomenon in Rocket Motors," AIAA Paper 80-1208, 1980.

[7] Mukunda, H. S., "A Comprehensive Theory of Erosive Burning in Solid Rocket Propellants," *Combustion Science and Technology*, Vol. 18, 1978, pp. 105-118.

[8] Ben Reuven, M. and Caveny, L. H., "Erosive Burning Theory for Propellants with Extended Flame Zones," AIAA Paper 80-0142, 1980.

[9] Razdan, M. K. and Kuo, K. K., "Erosive Burning Study of Composite Solid Propellants by Turbulent Boundary Layer Approach," *AIAA Journal*, Vol. 17, Nov. 1979, pp. 1225-1233.

[10] Beddini, R. A., "A Reacting Turbulent Boundary Layer Approach to Solid Propellant Erosive Burning," *AIAA Journal*, Vol. 16, Sept. 1978, pp. 898-905.

[11] Beddini, R. A., "Aerothermochemical Analysis of Erosive Burning in a Laboratory Solid-Rocket Motor," *AIAA Journal*, Vol. 18, Nov. 1980, pp. 1346-1353.

[12] Lengelle, G., "Model Describing the Erosive Combustion and Velocity Response of Composite Propellants," *AIAA Journal*, Vol. 13, March 1975, pp. 315-322.

[13] Rice, O. K. and Ginnell, R., "Theory of Burning of Double-Base Rocket Powders," *Journal of Physical Chemistry*, Vol. 54, 1950, pp. 885-917.

[14] Aoki, I. and Kubota, N., "Combustion Wave Structures of High and Low Energy Double-Base Propellants," AIAA Paper 80-1165, July 1980.

[15] Miller, R. R. and Foster, R. L., personal communication, Hercules/ABL, Aug. 1978; data generated under Contract F04611-78-C-0005.

[16] Beckstead, M. W., "A Model for Double Base Propellant Combustion," AIAA Paper 80-1164, July 1980.

[17] Kubota, N., Ohlemiller, T. J., Caveny, L., and Summerfield, M., "The Mechanism of Super-Rate Burning of Catalyzed Double Base Propellants," Princeton Univ. Aerospace and Mechanical Sciences Rept. No. 1087, March 1973.

[18] Glassman, I., *Combustion*, Academic Press, New York, 1977.

[19] Williams, F. A., *Combustion Theory*, Addison-Wesley Publ. Co., Reading, Mass., 1965.

[20] Burick, R. J. and Osborn, J. R., "Erosive Combustion of Double-Base Solid Rocket Propellants," CPIA Pub. 162, Vol. II, Dec. 1967, pp. 57-69.